JOURNAL OF MATERIALS SCIENCE 30 (1995) 3847–3852

Effect of sulphate removal on the surface texture and acid–base properties of TiO_2 (anatase)

C. MARTÍN, I. MARTÍN, V. RIVES*
Departamento de Química Inorgánica, Facultad de Farmacia, Universidad de Salamanca, 37007-Salamanca, Spain

Commercial anatase containing an appreciable amount of sulphur has been treated for sulphur removal by calcination at increasing temperatures or soaking with aqueous NaOH solutions. It has been found that both methods are active for sulphur removal, but the first one also leads to a sharp sintering of the titania particles. On the other hand, treatment with $NaOH_{aq}$ leads to incorporation of sodium cations. Both treatments lead also to changes in surface acidity, as measured by Fourier transform infrared (FT-IR) monitoring of pyridine adsorption.

1. Introduction

Titanium dioxide, both in the forms of anatase and rutile, is one of the most widely used metal oxides in industry; its high refractive index in the visible range permits preparation of thin films, and thus its use as a pigmentary material [1]. On the other hand, its use as a catalyst support for other oxides (V_2O_5, MoO_3, Cr_2O_3, etc.) or metals (Pt, Rh, etc.), or as a catalyst and photocatalyst itself is well known, acting not only as a support, but also interacting with the supported phase and thus acting as a promoter, developing the well-known strong metal-support interactions and also strong interaction with supported oxides, thus generally improving the selectivity of supported oxides in oxidation processes [2, 3].

It is already well known that catalytic properties, dispersion of the supported phase and photoactivity of these pigments, strongly depend on the presence of impurities, both in the bulk and/or the surface. Some of these impurities are usually introduced in the early stages of titania preparation (usually, chloride in rutile and sulphate in anatase); however, these impurities are sometimes added in order to improve the mechanical strength of the particles and their surface physicochemical or acid/base properties, by modifying the adsorption/desorption of the reactants/products, and thus affecting the activity and, mainly, the selectivity of these catalysts [4, 5].

Surface sulphate groups, either introduced to increase the activity [6] or from the preparative process [1] modify the Lewis acid–base properties of the titania surface. By calcination, sulphate is segregated and removed as volatile sulphur oxides [7, 8]. Alternatively, it can be also removed by reflux treatment with basic solutions. In the present paper, we report on the changes in the surface properties of titania (anatase) following removal of sulphate via these two methods. Both the surface texture (specific surface area and pore size distribution) and surface acid properties have been analysed.

2. Experimental procedure

2.1. Materials

Original titanium dioxide (hereafter sample C) was prepared by precipitation from titanyl sulphate and calcined at 720 K for 19 h. The sulphate contamination was equivalent to 7% SO_3.

2.2. Sample Preparation

Two methods were used in order to remove sulphate:
(i) Calcination in oxygen at 773, 873 and 973 K for 3 h, leading to samples C′, C″ and C‴, respectively.
(ii) Treatment with a 1 M NaOH aqueous solution. The procedure was as follows: 5 g of parent titania (sample C) were soaked in a shoxlet equipped with a reflux cooler containing 100 ml of aqueous NaOH (1 M) for 24 h at 323 K. The solid was filtered and washed until sodium was not detected in the washing liquids. The solid was then dried and calcined at 773 K in oxygen (sample C1). Two more samples were prepared by repeating once or twice the shoxlet and calcination treatments, leading to samples C2 and C3.

2.3. Characterization

Chemical analysis for sulphur and sodium was carried out by atomic absorption spectrometry in an ELL-240 apparatus, after disaggregation of the samples. X-ray diffraction (XRD) profiles were recorded in a Siemens D-500 instrument, equipped with a Difract-AT system and DACO-MP microprocessor; CuK_α radiation was used, with a graphite monochromator. Specific surface area and porosity assessment were carried out by

---

* Author to whom correspondence should be addressed.

0022–2461

nitrogen adsorption at 77 K in a conventional high vacuum system, equipped with a rotatory oil pump, silicon oil diffusion pump and a McLeod gauge for absolute pressure measurements; pressure chages were followed with MKS Baratron pressure transducer. Transmission electron microscopy (TEM) was performed in a Philips CM-10 instrument, between 40–100 kV; the samples were ultrasonically dispersed in acetone, the suspension being supported on a Cu grill impregnated with amorphous carbon.

Surface acidity was determined by pyridine adsorption as follows: pyridine was dried over a 0.3-nm molecular sieve and the adsorbate was degassed *in situ* with the freeze–pump–thaw technique prior to the adsorption runs. Adsorption was monitored by Fourier transform infrared (FT–IR) spectroscopy, using a Perkin-Elmer 16PC spectrometer, coupled to a conventional vacuum line; the sample was used in the form of a self-supported disc, in a specially designated cell with CaF_2 windows. The discs were previously activated *in situ* by calcination in air at 673 K for 2 h, and outgassed for 2 h at a residual pressure of about 10–3 $N m^{-2}$.

3. Results and discussion

3.1. Chemical Analysis

The results obtained, (summarized in Table I) indicate that, in samples treated by calcination in oxygen, the sulphur content is steadily decreased, from 2.8 to 0.23% as the calcination temperature is increased (from 720 to 973 K). For samples prepared by treatment with aqueous NaOH the results are rather similar, final sulphur content in the sample treated three times being 0.2%. Most probably, the very low sulphur percentage that is strongly held is forming some sort of titanium sulphate. Simultaneously, removal of sulphur by treatment with aqueous NaOH leads to an incorporation of sodium (see Table I).

3.2. X-ray Diffraction

The X-ray diffraction diagrams were coincident for all samples, despite the method followed to remove sulphur (increase of the calcination temperature of NaOH treatment). The profiles recorded for all samples show only the peaks due to diffraction by anatase planes, the most intense at 352 pm, corresponding to diffraction by the (1 0 1) planes; the only difference detected is the slightly wider broadness of the peaks in the profiles corresponding to samples prepared via the NaOH treatment, thus indicating a lower degree of crystallinity. It should be noted that in no case any peak due to diffraction by rutile planes is detected.

TABLE I Summary of chemical analysis (for S and Na) and specific surface areas of the samples studied[a]

Sample	Calcination temperature (K)	S^b	Na^b	S^c_{BET}	S^c_C	S^c_t
C	673	2.80	–	110	134	18.9 (t3) 115 (t1)
C′	773	1.20	–	51	84	22 (t3) 58 (t1)
C″	873	0.47	–	34	34	32
C‴	973	0.23	–	20	19	21
C1	773	0.80	0.07	65	65	63
C2	773	0.31	0.20	71	75	70
C3	773	0.20	0.30	73	74	73

[a] S_{BET} specific surface area determined by the BET method.
[b] wt %.
[c] $m^2 g^{-1}$.
S_C cumulative surface area;
S_t surface area determined by the *t*-method;

3.3. Textural Study

Specific surface areas of the samples are given in Table I. A sharp decrease in the specific surface area is observed in samples prepared by calcination, from 110 $m^2 g^{-1}$ for the sample calcined at 720 K, to 20 $m^2 g^{-1}$ for that calcined at 973 K. However, the NaOH treatment gives rise to a decrease, almost independent of the number of treatments given to the samples; the value is also lower than that for the sample calcined at the same temperature (773 K), but without the NaOH treatment. Such a decrease in the specific surface area as the calcination treatment is carried out at increasing temperatures cannot be related to a rutilization process, as no diffraction peak due to rutile was detected in the XRD profiles. So, such a change should be related to a modification in

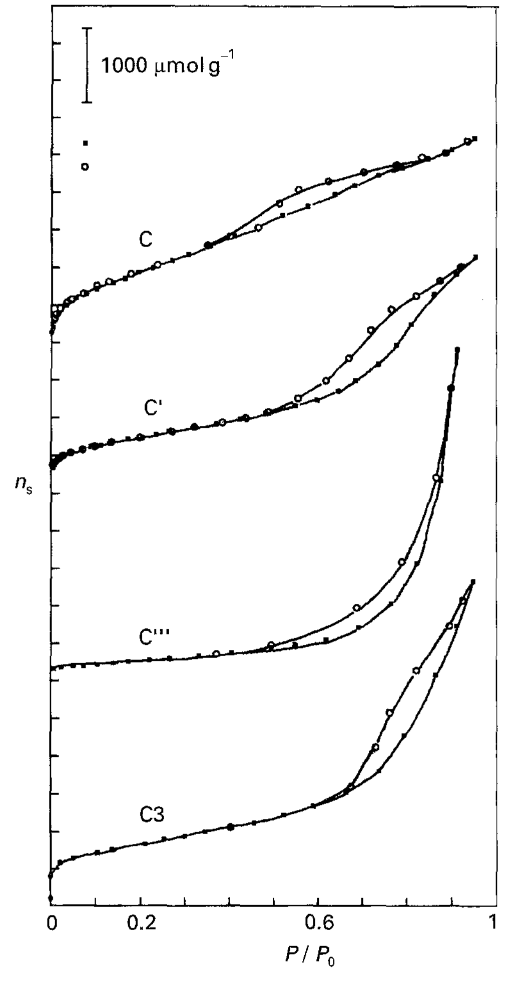

Figure 1 Nitrogen adsorption isotherms (77 K) of nitrogen on samples C, C′, C‴ and C3.

the morphology of the particles during the sintering process.

The nitrogen adsorption–desorption isotherms shown in Fig. 1 exhibit hysteresis loops in the $0.5 < P/P_0 < 0.9$ range, but a change is observed in the shape of these hysteresis loops. The adsorption branch for sample C is almost a straight line and the hysteresis loop corresponds to type E in de Boer's classification [9], being due to bottle-neck pores. On the contrary, all other samples (except sample C‴) show a type A hysteresis loop, due to cylindrical pores opened at both ends. The width of the hysteresis loop decreases as the amount of NaOH and the calcination temperature increase. The most intense changes are observed for sample C‴, where the hysteresis loop is rather narrow and a change in the shape of the isotherm is observed, now corresponding to type II in the IUPAC classification [10].

These changes are also detected in the pore size distribution in Fig. 2: while for sample C pores with an average diameter of 2–4 nm predominate, contribution to the surface area by these pores is rather low for sample C′, where a maximum contribution to the surface area arises from pores with a diameter of 5–6 nm. As the calcination temperature increases, contribution to the surface area by these pores with a diameter of 5–6 nm increases, but that by narrower pores (2–4 nm) decreases. When calcination is carried out at 973 K, pores with an average diameter close to 10 nm develop. On the contrary, for those samples treated under a basic medium, no change in the average diameter of the pores contributing to the surface area is observed.

Deviation in the values calculated for the specific surface area as determined following the method by Cranston and Inkley [11] are sometimes (samples C and C′) larger than those calculated by the Brunauer-Emmett-Teller (BET) method, probably due to condensation in the pores of these samples.

t-plots in Fig. 3 lead to straight lines passing through the origin, thus indicating the lack of microporosity in these samples. The curves are almost S-shaped, and from the slope of the first straight segment, the external S_{t1} areas have been calculated (see Table I). These results are essentially identical to those calculated by the BET method. When a well defined hysteresis loop is recorded (samples C and C′), three straight lines can be adjusted to the t-plot experimental data; in such a case the slope of the first line, S_{t1}, (that corresponding to the lowest t values) coincides with S_{BET}, while the cumulative surface area S_C coincides with the sum of the values calculated from the slopes of the first (S_{t1}) and the third (S_{t3}) straight segments. In other words, the external surface area still available after capillary condensation represented by the second segment is carried out from the slope of the third segment, S_{t3}.

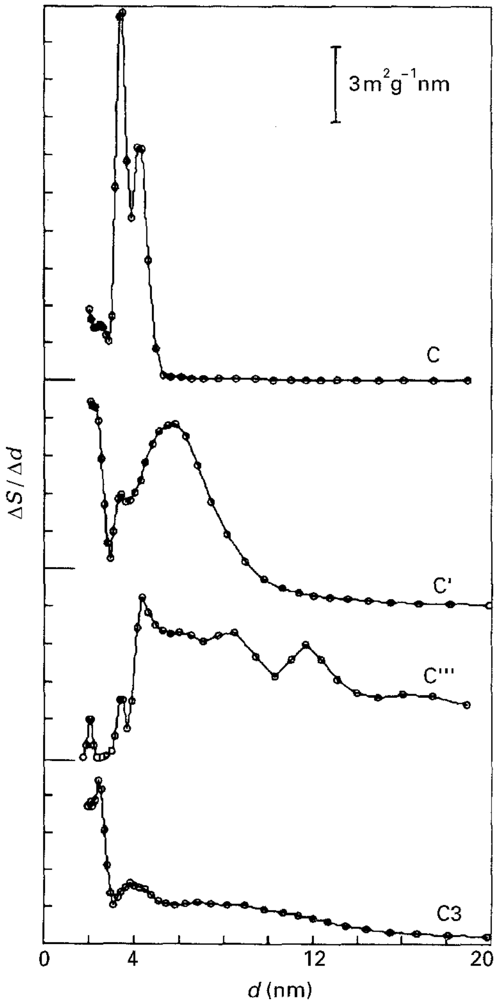

Figure 2 Pore size distribution curves for samples C, C′, C‴ and C3.

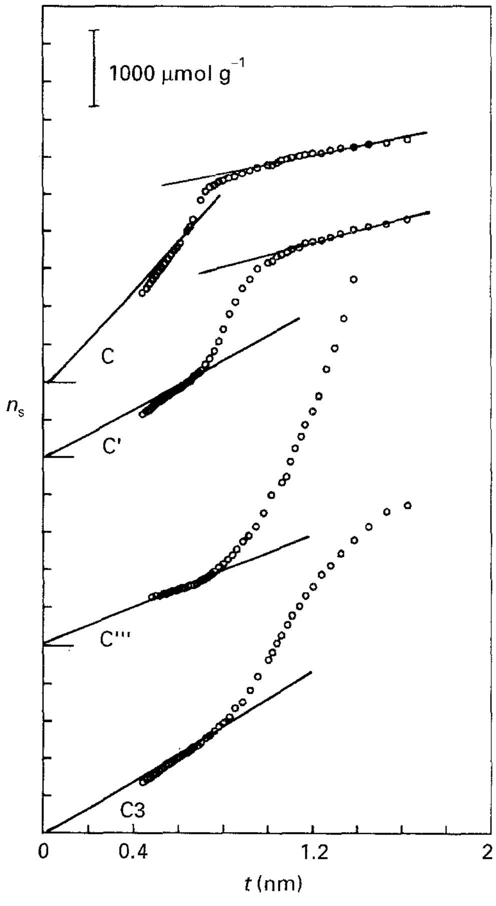

Figure 3 t-plots for samples C, C′, C‴ and C3.

3.4. Transmission Electron Microscopy

Morphological changes in these two sets of samples following the treatments given have been analysed by transmission electron microscopy (TEM). Important changes are only observed for samples where sulphate has been removed by high temperature calcination (Fig. 4). So while for sample C the sample is formed by very small particles, on increasing the calcination temperature larger homogeneous particles are observed (samples C′ and C‴); the average particle size corresponds to about 50 nm. Such a sintering is in agreement with the decrease in specific surface area above discussed (see data in Table I).

3.5. Surface Acidity

Adsorption of pyridine at room temperature and further outgassing at increasing temperatures, has been used to assess the effect of sulphate on the type (Lewis or Brönsted) and strength of the surface acid sites in these samples, and the changes undergone as sulphate is removed. Before adsorption of pyridine, the spectrum recorded for sample C shows a band at 1375 cm^{-1} due to ν_{SO} of covalently bonded surface sulphate species; its intensity decreases as the calcination or treatment with aqueous NaOH proceeds, and after calcination at 973 K (sample C‴) or at 773 K after two (sample C2) or three (sample C3) treatments with $NaOH_{aq}$, it is not recorded.

Adsorption of pyridine at room temperature on sample C, gives rise (Fig. 5a) to bands at 1447 and 1610 cm^{-1} due to stretching modes 19b and 8a of pyridine co-ordinated to surface acid Lewis sites (Table II), together with bands at 1541 and 1639 cm^{-1} due to modes 19b and 8a of protonated pyridine. The presence of both sets of absorption band reveals the presence, on this sample, of both Lewis and Brönsted acid sites (the latter being absent in undoped titania

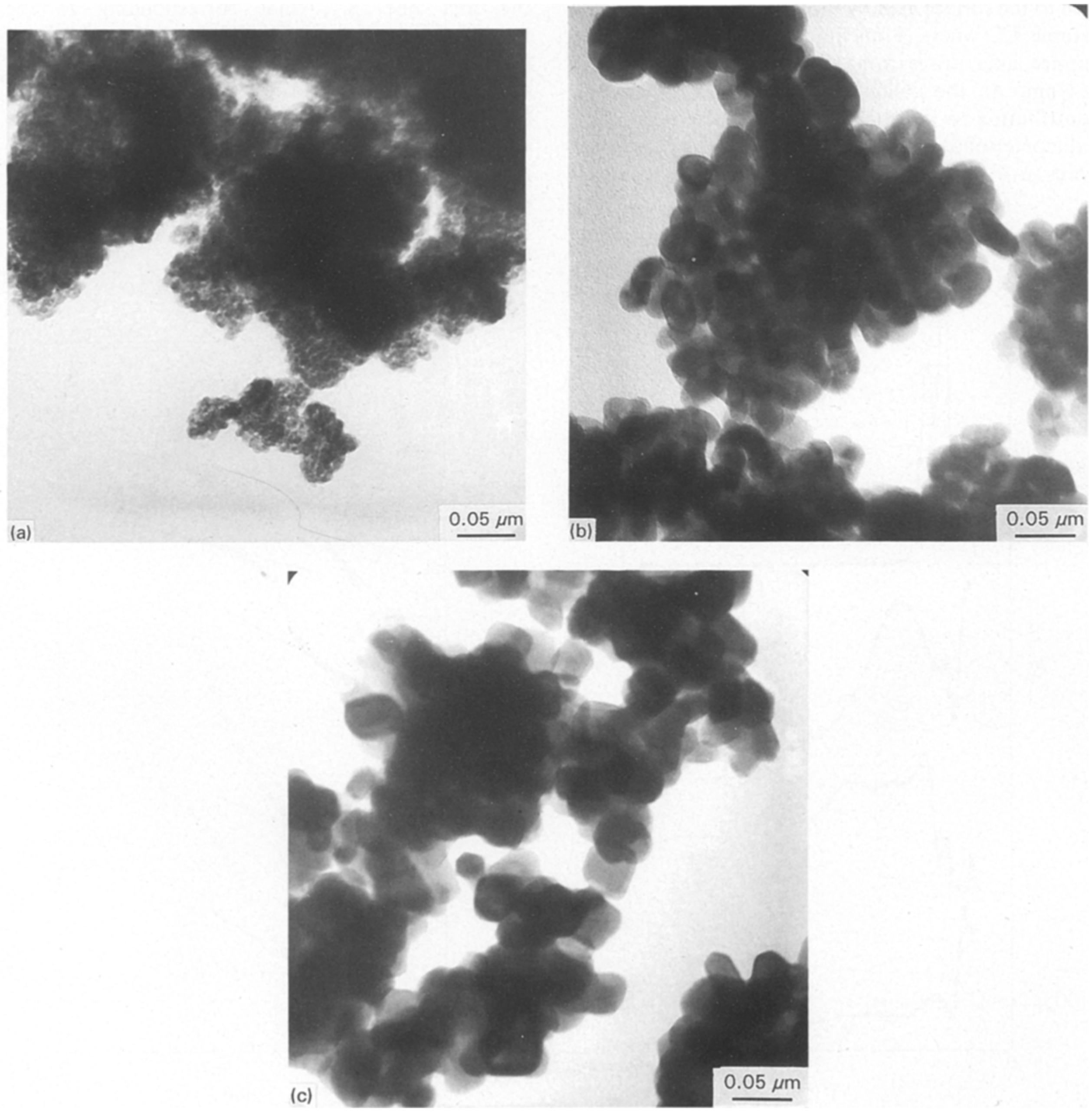

Figure 4 Transmission electron micrographs of samples (a) C, (b) C′, and (c) C‴.

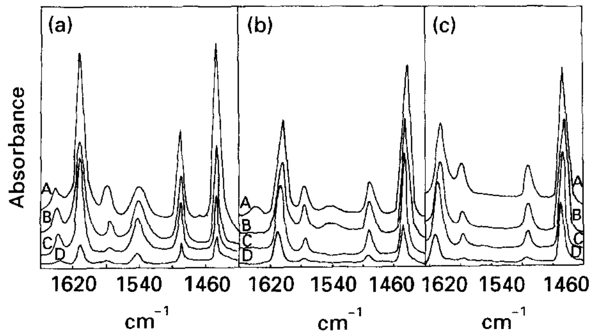

Figure 5 FT–IR spectra of pyridine adsorbed at room temperature and outgassed at (A) room temperature, (B) 373, (C) 473, and (D) 573 K on samples (a) C, (b) C′ and (c) C″ and C‴.

TABLE II Position (cm^{-1}) and adscription of the FT–IR bands recorded upon adsorption of pyridine at room temperature on the samples studied.

	Bpy			Lpy		
Sample	8a	19a	19b	8a	19a	19b
C	1639	1490	1541	1610	1490	1447 1438
C′	1640	1492	1540 (vw)	1603	1492	1444
C″	–	–	–	1603	1492	1444
C‴	–	–	–	1605	1490	1444
C1	–	–	–	1602 1590 (vw)	1492	1444
C2	–	–	–	1602 1590	1492	1443
C3	–	–	–	1603 1592	1492	1443

Bpy pyridine adsorbed on acid Brönsted sites.
Lpy pyridine adsorbed on acid Lewis sites.
vw very weak.

[12]). After outgassing at increasing temperatures the intensities of these bands are almost unchanged, even after outgassing at 673 K, thus indicating the adsorption sites correspond to very strong acid sites.

For sample C′, Fig. 5b, the same bands above described are recorded (Table II) although bands at 1640 and 1540 cm^{-1} due to modes 8a and 19b of pyridinium ion are rather weak. The other two samples corresponding to this same series (samples C″ and C‴) show rather similar spectra after pyridine adsorption, Fig. 5c, although bands due to pyridinium species are absolutely absent, thus indicating the lack of surface Brönsted acid sites in these samples. The remaining bands, due to pyridine co-ordinated to surface Lewis acid sites, shift to lower wave numbers (Table II). Thus, it should be concluded that increasing the calcination temperature, in addition to removing the surface Brönsted acid sites (probably related to removal of sulphate as sulphur oxides), also weakens the surface Lewis acid sites; even so, the bands corresponding to adsorption of pyridine on these sites are recorded even after outgassing at 673 K.

The behaviour shown by the samples treated in NaOH$_{aq}$ is rather different. For sample C1, Fig. 6a, as also observed for sample C′, no evidence is obtained on the existence of adsorbed pyridinium species (Table II), i.e. surface Brönsted acid sites do not exist on this sample, a fact probably related to removal of sulphate.

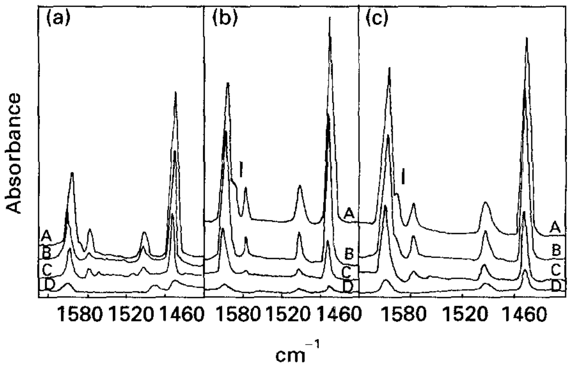

Figure 6 FT–IR spectra of pyridine adsorbed at room temperature and outgassed at (A) room temperature, (B) 373, (C) 473, and (D) 573 K on samples (a) C1, (b) C2 and (c) C3.

Bands due to coordinated pyridine are recorded at 1444, 1492 and 1602 cm^{-1}, also at lower wave numbers than for pyridine adsorbed on sample C. These findings, together with the decrease in the intensities of the bands (a decrease even stronger than that observed for sample C) as the outgassing temperature is increased, indicate a weakening of the strength of surface Lewis acid sites. It should be also noted that the FT–IR spectra of samples C2 and C3 show, upon pyridine adsorption, a new band at 1592 cm^{-1} (Table II) which intensity increases as the sodium content does (Fig. 6b, c). This band has been previously reported [13] for alkali ion-doped titania, and has been ascribed to adsorption of pyridine on co-ordinatively unsaturated Na$^+$ species. Nevertheless, these surface Lewis sites are rather weak, and the bands indicating their presence are removed after outgassing at 423–473 K.

4. Conclusions

The presence of sulphur in titania increases its surface acidity [14–16], as it develops surface Brönsted acid sites due to formation of hydrogensulphate ions (HSO_4^-). Surface Lewis acid sites are simultaneously strengthened, thus leading to superacid surface, which catalytic activity will be strongly modified.

Sulphate species can be removed as volatile sulphur oxides via high temperature calcination, or treatment with aqueous NaOH solutions and calcination at rather moderate temperatures. These two methods modify the surface texture of the samples (porosity) and, in addition, the first method also leads to a sharp sintering of the samples (i.e. a marked decrease in the specific surface area). On the other hand, treatment with NaOH$_{aq}$ solutions may lead to surface incorporation of new impurities (Na$^+$), although in a rather low concentration, but high enough to account for a modification of the surface acidic properties of the samples, developing new weak surface Lewis acid sites (co-ordinatively unsaturated Na$^+$ species) and weakening the strong surface Lewis acid sites originally existing on the surface (Ti^{4+} species). So, it should be concluded that although both methods success in elimination of sulphate, the right choice of one method or the other will depend on the ulterior application of the material.

Acknowledgements

The authors thank Dr. T. A. Egerton (Tioxide) for supplying the titania sample used in this study. I. M. acknowledges a grant from Ministerio de Educación y Ciencia (Madrid, Spain).

References

1. R. S. DARBY and J. LEIGHTON, in "The modern inorganic chemicals industry", edited by R. Thomson (The Chemical Society, London 1977) p. 354.
2. G. C. BOND and K. BRÜCKMAN, *Faraday Discuss. Chem. Soc.* **72** (1981) 235.
3. A. J. VAN HEGSTUM, J. G. VAN OMMEN, H. BOSCH and P. J. GELLINGS, *Appl. Catal.* **8** (1983) 369.
4. C. MARTÍN, I. MARTÍN. C. MENDIZABAL and V. RIVES, in "New frontiers in catalysis", Proceedings of the 10th International Congress on Catalysis, Budapest, Hungary, 1992, edited by L. Guzci, F. Solymosi, P. Tétény (Elsevier, Amsterdam, 1993) *Studies Surface Sci. Catal.* 1993, **75C**, 1987.
5. C. MARTÍN and V. RIVES, *J. Molec. Catal.* **48** (1988) 381.
6. G. BUSCA, H. SAUSSEY, O. SAUR, J. C. LAVALLEY and V. LORENZELLI, *Appl. Catal.* **14** (1985) 245.
7. C, MORTERRA, G. CERRATO, M. VISCA and D. M. LENTI, *Chem. Mater.* **3** (1991) 132.
8. F. GARBASSI, E. MELLO CERESA, E. OCHIELLO, L. POZZI, M. VISCA and D. M. LENTI, *Langmuir* **3** (1987) 173.
9. J. H. DE BOER, "The structure and properties of porous materials" (Butterworths, London, 1958).
10. K. S. W. SING, D. H. EVERETT, R. A. W. HAUL, L. MOSCOU, R. A. PIEROTTI, J. ROUQUEROL and T. SIEMINIEWSKA, *Pure Appl. Chem.* **57** (1985) 603.
11. R. W. CRANSTON and F. A. INKLEY, *Adv. Catal.* **9** (1957) 143.
12. H. MIYATA, Y. NAKAGAWA, T. ONO and Y. KUBOKAWA, *J. Chem. Soc., Faraday Trans. I* **79** (1983) 2343.
13. C. MARTÍN, I. MARTÍN C. del MORAL and V. RIVES, *J. Catal.* **146** (1994) 415.
14. K. TANABE, M. MISONO, Y. ONO and H. HATTORI, *Stud. Surf. Sci. Catal.* **51** (1989) 199.
15. T. YAMAGUCHI, *Appl. Catal.* **61** (1986) 104.
16. M. WAQIF, J. BACHELIER, O. SAUR and J.C. LAVALLEY, *J. Molec. Catal.* **72** (1992) 127.

Received 5 September 1994
and accepted 23 February 1995